Cell Biochem Biophys (2014) 68:615–628
DOI 10.1007/s12013-013-9757-7

ORIGINAL PAPER

Metabolic Alterations During the Growth of Tumour Spheroids

Katarzyna Bloch · Hannah Smith · Victoria van Hamel Parsons · David Gavaghan · Catherine Kelly · Alexander Fletcher · Philip Maini · Richard Callaghan

Published online: 14 September 2013

Abstract Solid tumours undergo considerable alterations in their metabolism of nutrients in order to generate sufficient energy and biomass for sustained growth and proliferation. During growth, the tumour microenvironment exerts a number of influences (e.g. hypoxia and acidity) that affect cellular biology and the flux or utilisation of fuels including glucose. The tumour spheroid model was used to characterise the utilisation of glucose and describe alterations to the activity and expression of key glycolytic enzymes during the tissue growth curve. Glucose was avidly consumed and associated with the production of lactate and an acidified medium, confirming the reliance on glycolytic pathways and a diminution of oxidative phosphorylation. The expression levels and activities of hexokinase, phosphofructokinase-1, pyruvate kinase and lactate dehydrogenase in the glycolytic pathway were measured to assess glycolytic capacity. Similar measurements were made for glucose-6-phosphate dehydrogenase, the entry point and regulatory step of the pentose-phosphate pathway (PPP) and for cytosolic malate dehydrogenase, a key link to TCA cycle intermediates. The parameters for these key enzymes were shown to undergo considerable variation during the growth curve of tumour spheroids. In addition, they revealed that the dynamic alterations were influenced by both transcriptional and posttranslational mechanisms.

Keywords Tumour metabolism · Solid tumour models · Warburg hypothesis · Glycolytic metabolism · Tumour growth · Tumour acidification · Metabolic adaptation

K. Bloch · D. Gavaghan · C. Kelly
Doctoral Training Centre, University of Oxford, Rex Richards Building, Parks Road, Oxford OX1 3QU, UK

H. Smith · V. van Hamel Parsons · R. Callaghan
Nuffield Department of Clinical Laboratory Sciences, John Radcliffe Hospital, University of Oxford, Oxford OX3 9DU, UK

C. Kelly
Department of Oncology, Gray Institute for Radiation Oncology and Biology, University of Oxford, Oxford OX3 7DQ, UK

A. Fletcher · P. Maini
Centre for Mathematical Biology, Mathematical Institute, University of Oxford, Oxford OX1 3LB, UK

R. Callaghan (✉)
Division of Biomedical Science and Biochemistry, Research School of Biology, College of Medicine, Biology and Environment, The Australian National University, Canberra, ACT 0200, Australia
e-mail: richard.callaghan@anu.edu.au

Introduction

Cellular metabolic processes provide sufficient energetic and anabolic capacity to maintain growth, repair and overall integrity. Typically, the production of energy consists of near complete oxidation of glucose and fatty acids; two of the primary metabolic fuels. Cancer cells display a heavy reliance on the glycolytic pathway for their energetic needs, with a significant dampening of the mitochondrial oxidative phosphorylation route [1, 2]. Initial hypotheses suggested that cancer cells have impaired mitochondrial function, but this was subsequently disproven, and moreover, the TCA cycle continues in its anaplerotic provision of biosynthetic precursors [3–7]. The reason for this reliance on glycolysis has also been attributed to lack of available oxygen, the terminal electron acceptor. In specific tumour regions (i.e. distal to blood supply), this is a highly plausible suggestion. However, it has also been shown that

the glycolytic reliance remains even under conditions of sufficient oxygen provision [8, 9]. It appears that cancer cells adopt a "programmed" switch to a greater reliance on the less efficient glycolytic pathway for energy.

Such a strategy seems contradictory to the seemingly high-energy requirements of cancer cells, illustrated by their invasiveness and high rates of proliferation. However, it is worth considering that proliferating cancer cells do not aim to maximise ATP yield from the metabolism of fuels [2, 6]. There is also an imperative to provide sufficient biomass (i.e. protein, lipid and nucleotide) for cellular replication. This should be considered a primary objective of metabolic function in proliferative tissue, and the supply of ATP is directed to sustain the anabolic capacity. Clearly, proliferating cancer cells direct metabolic pathways in a distinct manner to healthy cells. Control of metabolic flux is a complex process involving both short- and long-term pathways and may be directed via cellular demand and inter-cellular signalling.

Substrate availability and the cellular metabolic ratio (i.e. [ATP]/[ADP] and [NADH]/[NAD^+]) are the primary short-term drivers for the direction of metabolic flux. The ratios of these key metabolic intermediates reflect the cellular redox status and they direct metabolic flux towards the provision of energy or formation of storage products for future utilisation. Typically, their effects on metabolic flux are via allosteric regulation of enzyme activity, which is a rapid response pathway.

Modulation of enzyme expression levels is another important route in controlling metabolic flux within cancer cells. In addition to tumour suppressors such as p53, the oncogenes c-Myc and hypoxia inducible factor-1 (HIF-1) have been widely implicated in the modulation of tumour metabolism [2, 10, 11]. c-Myc and HIF-1 encode transcription factors that activate or repress expression of vast numbers of genes. Altered regulation or function of c-Myc is a common abnormality in cancer and has been associated with perturbations in the metabolism of nucleotides, glucose and glutamine [12, 13]. The HIF-1 transcription factor is a dimer of HIF-1α and HIF-1β subunits. The β-subunit is constitutively expressed, whilst the stability of the α-subunit is greatly increased under conditions of hypoxia or anoxia [14]. The inevitable regional hypoxia in solid tumours means that HIF-1 plays a prominent role in hypoxic regions of tissues. Amongst a large number of target genes, HIF-1 is known to control expression of genes involved in glucose uptake, the glycolytic pathway, the TCA cycle and glutamine consumption [15–17]. In addition, mutations in the tumour suppressor p53 also regulate numerous aspects of cell metabolism including mitochondrial oxidative phosphorylation, glucose metabolism, glutamine utilisation and the pentose-phosphate pathway [18–20].

Tumour growth is associated with the presence of a harsh microenvironment that will impart a number of specific influences on the cellular control mechanisms for metabolism. Oxygen gradients are well established within tumours, and cellular access to adequate oxygen is related to proximity of tumour or host vasculature [21]. Production of lactate and CO_2 through metabolism results in the acidification of the interstitial space [22, 23]. Solid tumour architecture also generates high cell–cell contact and a resultant increase in hydrostatic or interstitial pressure [24, 25]. These factors preclude the efficient removal of metabolic toxins and contribute to the intra-tumoral gradients of oxygen, growth factors and nutrients. Cells proximal to the vasculature will avidly utilise nutrients at considerable expense to those in the deeper locations of a solid tumour. The harsh microenvironment is a major contributor to the establishment of distinct zones of cell types within a tumour. These include variations in proliferative capacity, oxygenation status and even the presence of necrotic cells. Variations in these cellular types and zones will occur during the growth of solid tumour tissue.

In the present investigation, the tumour spheroid model was used to investigate glucose metabolism. The tumour spheroids progress through a number of stages during their growth period from small tissue diameter with predominantly normoxic and proliferative cells through to large tissue diameter with the emergence of a significant population of quiescent and/or hypoxic cells. These variations in cell type will influence the utilisation of glucose through catabolic routes to provide cellular energy or biomass according to specific need. In the present investigation, the protein expression profiles for a number of enzymes involved in glucose catabolism were examined; in particular those within glycolysis and the pentose-phosphate pathway (PPP). Moreover, the overall metabolic capacity of these enzymes was measured throughout the growth of tumour spheroids. The spheroids were also grown under conditions to exacerbate the deprivation of metabolic fuel and the production of an acidic environment.

Materials and Methods

Materials

RPMI-1640 medium (with L-glutamine and 25 mM HEPES), foetal bovine serum, penicillin and streptomycin were purchased from Invitrogen Ltd. (Paisley, UK). Glucose-6-phosphate dehydrogenase, lactate dehydrogenase, phosphoenolpyruvate, sodium pyruvate, oxaloacetic acid and glucose-6-phosphate were obtained from Sigma-Aldrich (Dorset, UK). The DC protein assay was purchased from Bio-Rad Laboratories Ltd. (Hemel Hempstead, UK),

and the lactate assay kit was obtained from Megazyme International (Wicklow, Ireland). EDTA-free protease inhibitor tablets (Complete) were purchased from Roche Diagnostics Ltd. (Burgess Hill, UK). The reduced and oxidised forms of β-nicotinamide-adenine dinucleotide and β-nicotinamide-adenine dinucleotide phosphate (NADP) were purchased from Merck Chemicals Ltd. (Nottingham, UK). Primary antibodies to glucose-6-phosphate dehydrogenase (anti-rabbit), hexokinase (anti-rabbit), pyruvate kinase (HRP-linked, anti-goat) and lactate dehydrogenase (HRP-linked, anti-goat) were purchased from Abcam (Cambridge, UK). The secondary polyclonal HRP-conjugated antibodies were also obtained from Abcam. The anti-phosphofructokinase-1 antibody was from Santa Cruz Biotechnology (Heidelberg, Germany).

Cell Culture and Tumour Spheroid Growth

DLD-1 human colon carcinoma cells were obtained from Dr. Roger Phillips (University of Bradford, UK) and grown as monolayer cultures in RPMI-1640 medium containing glutamine and supplemented with 10 % (v/v) foetal calf serum and penicillin/streptomycin (100 IU mL^{-1} and 100 mg mL^{-1}, respectively).

To generate tumour spheroids, trypsinised cell monolayers were transferred to 75-cm^2 flasks containing a base coat of 0.75 % (wv^{-1}) agarose in serum-free medium. The flasks were left for 24 h, and cell aggregates were then added to two 500-mL spinner flasks in a total volume of 100 mL and stirred at 55 rpm (Techne MCS-1045) at 37 °C, 5 % CO_2. Over the following 20-day growth period, the medium in one flask was changed every 48 h, and therefore, the glucose levels were supplemented; termed "*high nutrient*" conditions. Spheroid density was maintained at a constant level throughout the culture period. In the other flask, the medium was not changed, and therefore, glucose levels became depleted; referred to as "*low nutrient*" conditions.

Tumour spheroids generated from DLD1 cells have been extensively characterised for proliferative status, quiescence, hypoxia and growth characteristics in previous publications [26–28]. To measure the ability of hypoxia to induce expression of c-Myc and Hif-1 in tumour spheroids, the tissue was grown as previously described [28].

Tumour Spheroid Homogenate Preparation

In order to measure metabolic enzyme capacity, spheroid homogenates were prepared at a series of times during the 20-day growth period. Aliquots of spheroids were collected from the spinner flasks and the medium discarded. The spheroids were homogenised extensively using disposable mini-homogenisers in centrifuge tubes with buffer containing 50 mM Tris–HCl pH 8.0 and 13 mM $MgSO_4$. Unbroken cells and debris were removed by centrifugation (3,000*g*, 5 min), and the homogenates were dispensed into 50 μL aliquots and flash frozen in liquid nitrogen for storage at −80 °C. A total protein assay kit (DC Bio-Rad) with BSA as a standard was used to determine the concentration of protein in each spheroid homogenate.

Measurement of pH, Lactate and Glucose in Culture Medium

Every 24 or 48 h, a 1 mL aliquot of spheroids was removed from the spinner flasks for size determination. The medium was decanted, and the spheroids suspended in 1 mL phosphate-buffered saline. A graduated calibrated microscope eyepiece graticule (Pyser-SGI, UK) was used to measure the diameter of the spheroids. The measurement was converted into micrometres (μm), which was used to calculate the volume of the TS (mm^3). The growth data were fitted using the exponential curve:

$$Y = A \times e^{kt}$$

where Y = spheroid volume (mm^3), A = constant, t = time (days) and k = rate constant.

A mini electrode was used to measure pH in the decanted 1 mL sample of medium from both the spheroid spinner flasks. The medium samples were immediately flash frozen with liquid nitrogen and stored at −80 °C.

Glucose levels in the samples were measured in an ADVIA 2400 (Bayer, UK) analyser to detect extracellular glucose using the reagents from Roche (Mannheim, Germany). These measurements were kindly performed by the NHS Department of Clinical Biochemistry (John Radcliffe Hospital, Oxford, UK).

A commercial assay kit (Megazyme) was used to determine the concentration of lactate in the samples. The medium samples (1 mL) were deproteinised by adding 200 μL of ice-cold 1 M perchloric acid. The sample was mixed by vortex and subsequently centrifuged at 1,500*g* for 10 min; the supernatant was removed, and the process was repeated. The supernatant was neutralised by the addition of 200 μL 1 M KOH. Lactate was measured according to the supplier's instructions using a spectrophotometric method.

Measurement of Enzyme Activity in Tumour Spheroid Homogenates

The activities of a series of cytosolic metabolic enzymes were measured in the TS homogenates using colorimetric assays. Each of the reactions was coupled to the oxidation or reduction in the cofactors NAD^+/NADH or $NADP^+$/NADPH. The appearance or disappearance of NADH (or

NADPH) was measured continuously in a dual-beam Hitachi U-2010 spectrophotometer using a wavelength of 340 nm at 37 °C. The cuvette volumes were 1 mL, the blank cuvette contained components other than homogenate, and the reactions were started by the addition of 100 μg homogenate protein. Enzyme activities were expressed as μmoles of NADH utilised (or formed) per minute per mg of homogenate protein.

The hexokinase assay buffer contained 0.05 M Tris–HCl pH 8, 13.3 mM $MgSO_4$, 0.55 mM Na_2ATP, 0.22 mM $NADP^+$, 20 mM glucose and 1.5 U/mL glucose-6-phosphate dehydrogenase.

The pyruvate kinase (PYK) assay buffer contained 0.05 M Imidazole–HCl pH 7.6, 0.12 M KCl, 0.062 M $MgSO_4$, 1.48 mM Na_2ADP, 0.218 M NADH, 0.2 mg/mL lactate dehydrogenase and 3 mM phosphoenolpyruvate.

The lactate dehydrogenase assay buffer contained 0.2 M Tris–HCl pH 7.3, 0.218 M NADH and 4 mM sodium pyruvate.

The glucose-6-phosphate dehydrogenase assay buffer contained 0.055 M Tris–HCl pH 7.8, 0.0033 mM $MgSO_4$, 0.2 mM $NADP^+$ and 0.02 M glucose-6-phosphate.

The phosphofructokinase-1 assay buffer contained 50 mM Tris–HCl pH 7.6, 5 mM $MgSO_4$, 5 mM NH_4SO_4, 0.35 mM fructose-6-phosphate, 0.1 mM Na_2ATP, 0.25 mM NADH, 2.5 U triose-phosphate-isomerase, 1.5 U aldolase and 3.6 U glycerophosphate dehydrogenase.

The malate dehydrogenase assay buffer contained 0.1 M glycine adjusted to pH 10 with NaOH, 0.12 M malate and 2 mM NAD^+.

Measurement of Enzyme Expression Levels

The relative expression level of each enzyme during the growth period for the spheroids was determined using Western immunoblotting. Total proteins in homogenate samples were resolved using SDS-poly-acrylamide gel electrophoresis [monocratic gels between 6 and 12 % (w/v)]. Samples were heated in Laemmli sample buffer for 10 min at 90 °C prior to electrophoresis.

Specific conditions of dilution, blocking buffer and secondary antibody (where required) were done according to the manufacturers recommendations. Detection was achieved using chemiluminescence using HRP-conjugated primary or secondary antibody. Densitometric analysis, performed with Image J, was used to determine the relative expression levels of each enzyme. The value at 2 days was assigned a value of 1.0 and sample intensities normalised accordingly.

Data Analysis

Enzyme activity assays were analysed using linear regression of the spectrophotometric data, and the growth curve was fitted using nonlinear least squares regression. These analyses were carried out using the GraphPad Prism 4 program. Multiple comparisons of mean data were done using one-way ANOVA and post hoc analysis using Bonferroni's multiple comparison test.

Results

Overall Metabolic Capacity of Tumour Spheroids Across the Growth Curve

Spheroids comprising DLD-1 cells were grown under two distinct conditions; one with medium replenishment every 48 h, referred to as *high nutrient* conditions. The glucose concentration of the medium was 11.1 mM and the pH set at 7.44. The other growth condition did not have medium replenishment during the 20-day period of growth; referred to as *low nutrient* conditions. It has previously been shown that DLD-1 spheroids may be grown for a period of 21–24 days, at which point their diameter reaches 1,000 μm [26]. At this point, the central region of the spheroid is necrotic, and the structural pressures within the tissue lead to collapse and fragmentation. Observations were done throughout the growth curve of spheroids in order to encompass the full range of microenvironment factors that shape metabolism (i.e. hypoxia, low pH, etc.). The ability to reproduce this extent of factors is not achievable using a 2-D (monolayer) culture system [29].

The growth of spheroids was assessed by sampling the tissues, and the diameter converted to a volume. At all stages of the growth curve, the spheroid volume was greater for the high nutrient conditions (Fig. 1a). This indicates that deprivation of fresh metabolic fuels, and presumably the failure to remove toxic metabolites, resulted in impaired growth of the spheroids. By final day, the tissue volume was 7.5-fold greater in the high (2.12 ± 0.10 mm^3) than the low (0.282 ± 0.066 mm^3) nutrient growth conditions.

Figure 1b shows the amount of glucose consumed from the culture medium in successive 48-h periods; in the high nutrient model, the glucose levels were replenished to 11.11 mmol/L (i.e. 1.11 mmol per 100 mL). The glucose concentration in the culture medium under low nutrient conditions decreased during the growth period, and the amount of glucose consumed from the culture medium fell progressively. By day 16, the data indicated near negligible levels of glucose consumption. Under high nutrient conditions, the consumption of glucose in each 48-h period rose throughout the growth period examined. This was particularly evident during the most rapid growth phase of the TS (i.e. days 10–15). By day 20, the spheroids had consumed 0.88 mmol of the 1.11 mmol (i.e. 80 %) glucose

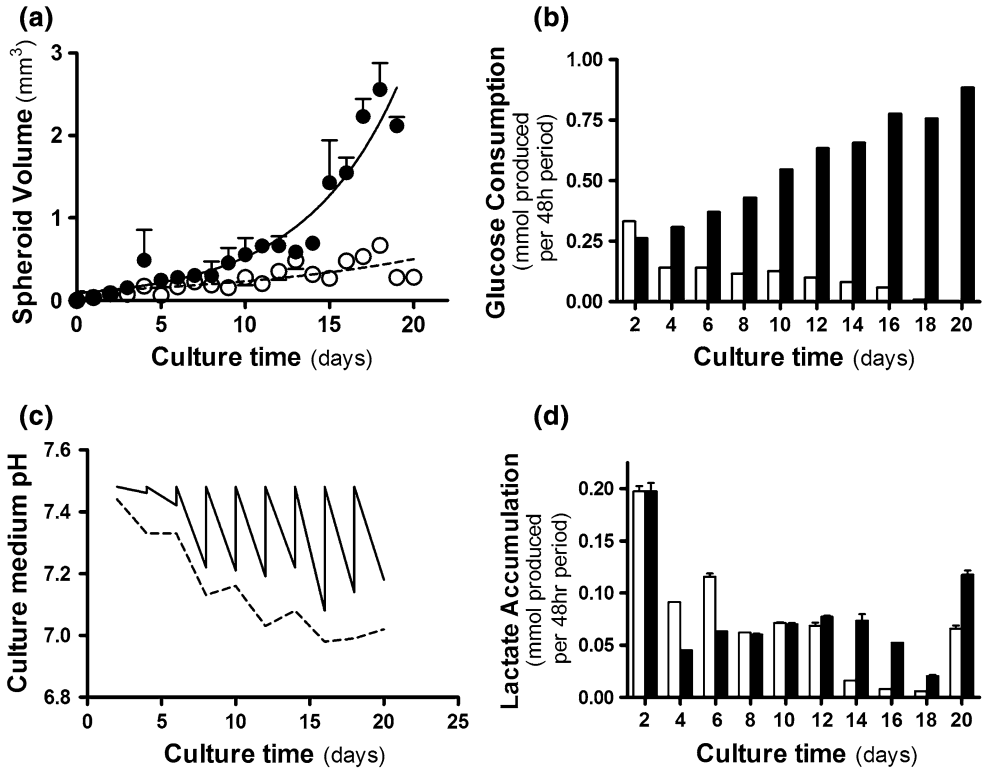

Fig. 1 Growth and overall metabolic characteristics of TS. **a** Tumour spheroids comprising DLD-1 cells were grown under two distinct conditions; with medium replenishment every 48 h (*filled circle*), or, with no replenishment (*open circle*) over the 20-day growth period. Each day a small fraction (1 mL) from each growth condition was used to estimate spheroid growth. The diameter from at least 10 spheroids was measured using an eyepiece graticule and converted to tissue volume. Each data point (mean ± SEM) represents measurements from at least five independent spheroid cultures. **b** Glucose concentration was measured in 1 mL aliquots at 48-h intervals during the 20-day growth period of the spheroids. The concentration was used to ascertain the amount of glucose consumed in the previous 48-h period and expressed as μmoles of glucose produced per 48-h period. Data were obtained for spheroid cultures under low nutrient (*open square*) or high nutrient (*filled square*) conditions and represent the mean of triplicate measurements. **c** The pH of the culture medium was measured in 1 mL aliquots at 48-h intervals during the 20-day growth period of the spheroids. Data were obtained for spheroid cultures obtained under low nutrient (*dashed line*) or high nutrient (*solid line*) conditions and represent the mean of triplicate measurements. **d** Lactate was measured in 1 mL aliquots at 48-h intervals during the 20-day growth period of the spheroids. The concentration was used to ascertain the amount of lactate accumulated in the medium during the previous 48-h period and expressed as μmoles produced per 48-h period. Data were obtained for spheroid cultures obtained under low nutrient (*open square*) or high nutrient (*filled square*) conditions and represent the mean ± SEM of three independent spheroid cultures

available in the 100 mL culture, and the availability of nutrient fuel could be classed as limiting.

During the 20-day growth period, the pH of the medium in low nutrient conditions fell gradually from 7.44 to 7.02 by day 20 (Fig. 1c), which represents a near threefold increase in $[H^+]$. This increase in the acidity occurred despite the considerable buffering capacity of the culture medium, which contains 25 mM HEPES and 23 mM $NaHCO_3$. A more complex decay of the medium pH was observed in the high nutrient conditions. Replenishment of the culture medium every 48 h returned the pH to 7.44. Each of these 48-h periods was associated with a considerable drop in the pH, typically of 0.2 pH units. This continued acidification of the medium broadly followed the glucose consumption rate shown in Fig. 1b.

Acidification of the medium is brought about by several factors and two of the major influences being the generation of CO_2 (and therefore H_2CO_3) by respiring tissues and the production of lactic acid by oxygen deprived cells. Lactate production is generally considered the primary source of acidification in tumours due to the heavy reliance on glycolytic metabolism for energy production and ability of this pathway to generate intermediates for anabolic pathways. High lactate production was observed, and equivalent for both culture conditions, in the first 48 h of growth (Fig. 1d) and presumably reflects the metabolic demands during the formation of the solid tissue mass. Until day 6, the level of lactate production in low nutrient conditions was significantly greater. In the period from days 6 to 12, the two growth conditions displayed near

identical rates of lactate production. From day 12 to day 18, lactate production was almost negligible in the low nutrient conditions; which presumably reflects the absence of any significant glucose for oxidation in the glycolytic pathway. In the same period, spheroids grown in high nutrient conditions retained significant lactate production reflecting the continued glycolytic metabolism sustained by continued replenishment of glucose. At day 20, both culture conditions displayed a sudden rise in lactate production; however, at this time, the tissues have reached near maximum growth and contained considerable necrotic tissue.

Whilst the glucose (or nutrient) deprivation strategy may not be a "physiological" condition, it does provide a considerable metabolic stress on the spheroids. The lack of glucose and glutamine presents deficiency of essential nutrients, and the failure to remove "spent" medium will ensure the build-up of metabolic waste products, elevated ammonia and acidic pH. These factors are typical of those encountered by solid tumours due to the lack of an efficient vasculature.

Tumour spheroids provide an excellent system of considerable complexity to investigate cancer biology by reproducing many observations found in vivo. For example, the production of hypoxia in TS leads to increased stabilisation of the expression of Hif-1a and c-Myc proteins (Fig. 2) and reveals that the spheroid model is associated with the actions of these well-described proteins.

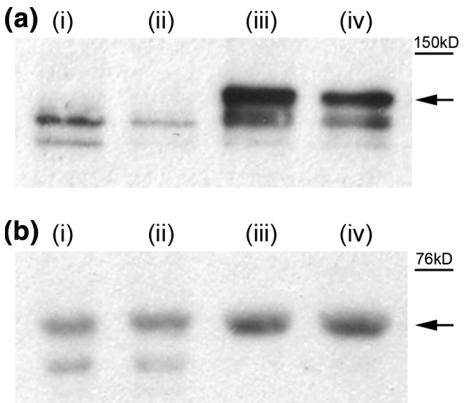

Fig. 2 Expression of Hif-1 and c-Myc in hypoxic tumour spheroids. Tumour spheroids were grown under normoxic conditions or subjected to a 16-h period of hypoxia. Expression of the transcription factors Hif-1 and c-Myc was measured using Western immunoblotting. **a** Expression of Hif-1 in tumour spheroids grown under normoxic (*lanes i–ii*) or hypoxic (*lanes iii–iv*) conditions. Samples (10 μg per lane) were analysed by 10 % SDS-PAGE, the *arrow* indicates Hif-1, and the *line* corresponds to a molecular weight of 150 kD. **b** Expression of c-Myc in tumour spheroids grown under normoxic (*lanes i–ii*) or hypoxic (*lanes iii–iv*) conditions. Samples (10 μg per lane) were analysed by 8 % SDS-PAGE, the *arrow* indicates c-Myc, and the *line* corresponds to a molecular weight of 76 kD

Maximal Activity Capacity and Expression of Hexokinase and Phosphofructokinase-1 During Tumour Spheroid Growth

The glucose consumption, lactate production and the acidification of the culture medium strongly support high rates of glycolytic metabolism in the spheroids. This was sustained throughout the growth curve of spheroids under high nutrient conditions. In contrast, the low nutrient conditions rendered glycolysis ineffective to support tissue growth due to depletion of glucose.

We have investigated the capacity of spheroids to mediate several key reactions of the glycolytic pathway. The first two reactions involve (1) hexokinase to trap glucose within cells as glucose-6-phosphate and (2) PFK-1, which is the highly regulated enzyme that commits glucose to entry into the glycolytic pathway.

As shown in Fig. 3a, c, the activity and expression levels for hexokinase were markedly different between the low and high nutrient growth conditions. In the low nutrient conditions, the activity of hexokinase remained steady for the first 16 days of culture. During this period, there was, however, a gradual decline in the overall expression levels of hexokinase II. Rather surprisingly, there was an elevation of hexokinase activity in the last 4 days of culture despite the reduction in overall expression. This may reflect altered posttranslational modification or regulation of the hexokinase enzyme. Alternatively, it may indicate that an enzyme other than hexokinase II (e.g. HK1) is compensating.

During the initial 6 days of growth, the hexokinase activity in spheroids with high nutrient availability also remained steady and did not differ from the nutrient depleted spheroids. This was likely due to the fact that glucose levels had not been exhausted by this time in the low nutrient conditions. Between days 6 and 15, the hexokinase capacity was significantly higher in the spheroids grown in high nutrient conditions. This period also corresponded to one of high glucose consumption and lactate production (see Fig. 1). However, the relative expression levels of hexokinase II rose marginally, but not to a statistically significant level. This suggests that the increased hexokinase capacity was bought about by modified regulation of the available enzyme.

PFK-1 mediates the conversion of fructose-6-phosphate to fructose-1,6-bis-phosphate; the reaction requiring ATP hydrolysis and fully commits glucose to the glycolytic pathway. Moreover, PFK-1 is one of the most highly regulated enzymes in the glycolytic pathway, responding to hormonal influences and cellular redox status.

The capacity of PFK-1 in spheroids did not alter in overall activity or differ between high and low nutrient growth conditions during the first 10 days of culture (Fig. 3b, d). Under high nutrient conditions, the capacity of

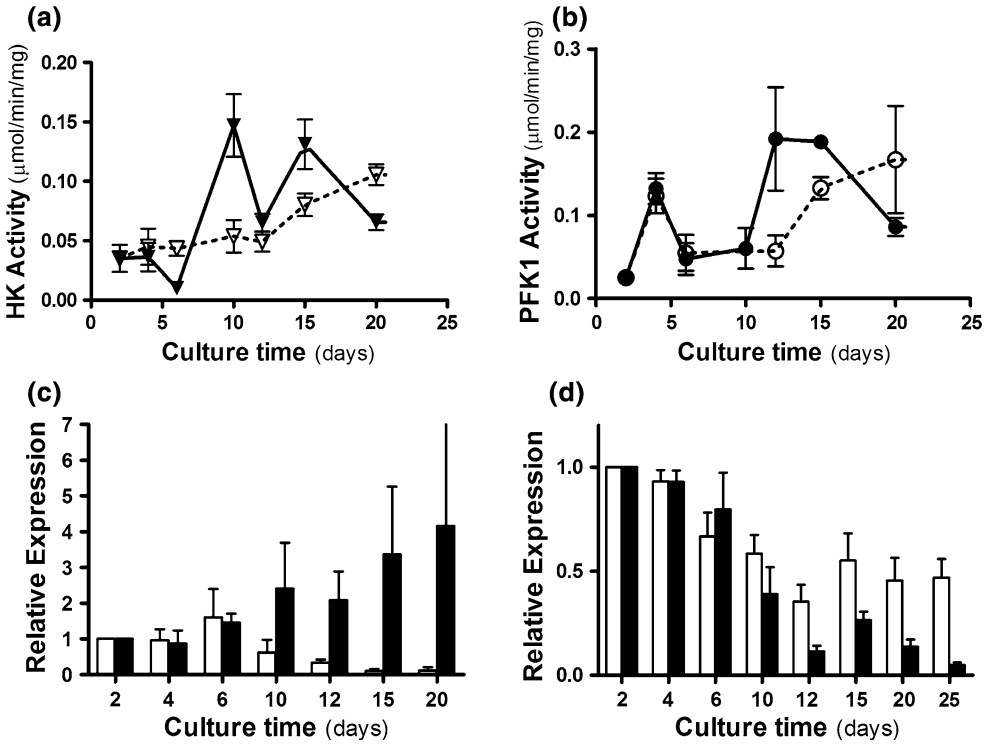

Fig. 3 Activities and expression levels of enzymes involved in glycolytic entry. The activities of **a** hexokinase and **b** phosphofructokinase-1 were measured at the times indicated in the growth curve of spheroids grown under low (*open circle*) or high (*filled circle*) nutrient conditions. Enzyme activities were determined using coupled assay systems and spectrophotometric determination of NAD(P)H appearance or utilisation. The spectrophotometric data were expressed as μmol/min/mg protein. The relative expression levels of **c** hexokinase and **d** phosphofructokinase-1 were measured at the times indicated in the growth curve of spheroids grown under low (*open square*) or high (*filled square*) nutrient conditions. Expression levels were obtained using Western immunoblotting of spheroid homogenates and normalised to the value obtained at day 2 (assigned as 1.0). All data points correspond to the mean ± SEM obtained from at least three independent spheroid homogenates

PFK-1 rose dramatically between days 10 and 15 and then fell sharply until day 20. The expression of PFK-1 under high nutrient conditions did not reflect this pattern; in fact, the overall amount of enzyme dropped during this period of high glucose consumption (see Fig. 1).

Under low nutrient conditions, there was a similar pattern for the capacity of PFK-1, although the increase did not occur until 12 days of culture (Fig. 3b, d). However, the amount of enzyme expressed in the tissue did not alter from days 8 to 20. In addition, the amount of PFK-1 was consistently higher in spheroids grown under low nutrient compared to high nutrient conditions. Presumably, the modification of capacity and expression patterns reflect altered regulation of enzyme activity to optimise the scavenging of any available nutrient fuels.

Maximal Activity Capacity and Expression of Pyruvate Kinase and Lactate Dehydrogenase During Tumour Spheroid Growth

The conversion of phosphoenolpyruvate to pyruvate results in the liberation of ATP and is the final reaction in glycolysis. The reaction is catalysed by pyruvate kinase, which is subjected to extensive regulation within the cell. Pyruvate kinase is activated by fructose-1,6-bisphosphate and inhibited by both ATP and alanine. In addition, the enzyme undergoes hormonally directed phosphorylation–dephosphorylation cycles. This key final step in glycolysis controls the flow of intermediates towards provision of biosynthetic precursors or the production of ATP.

The activity of pyruvate kinase did not alter significantly during the 20-day growth period under low nutrient conditions (Fig. 4a). This finding was directly correlated with the cellular expression levels of the enzyme, which were also unaltered during the growth period examined (Fig. 4c). Under high nutrient conditions, the cellular capacity of pyruvate rose from day 4, to a maximum value at 12 days, and then dropped back to the initial level by day 20. The rise in capacity to day 12 correlated with the increase in glucose consumption during this period, suggesting that the oxidation of glucose was utilised in energy provision. Between days 12 and 20, the glucose consumption rose, whereas the capacity of pyruvate kinase fell. This inverse relationship may suggest that glucose was

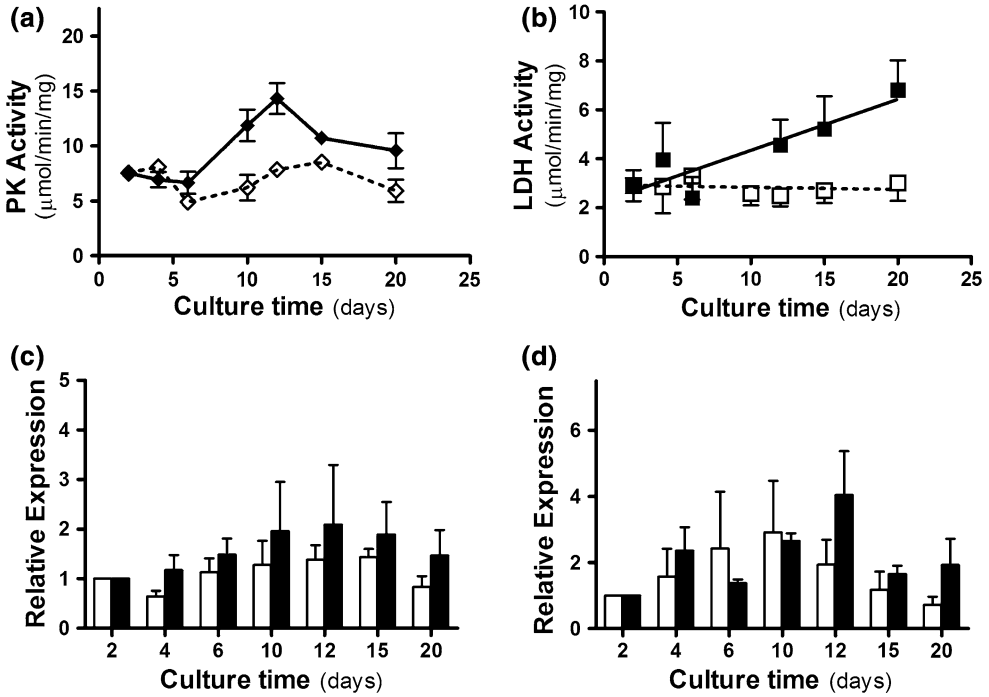

Fig. 4 Activities and expression levels of enzymes involved in glycolytic exit. The activities of **a** pyruvate kinase and **b** lactate dehydrogenase were measured at the times indicated in the growth curve of spheroids grown under low (*open circle*) or high (*filled circle*) nutrient conditions. Enzyme activities were determined using coupled assay systems and spectrophotometric determination of NAD(P)H appearance or utilisation. The spectrophotometric data were expressed as μmol/min/mg protein. The relative expression levels of **c** pyruvate kinase and **d** lactate dehydrogenase were measured at the times indicated in the growth curve of spheroids grown under low (*open circle*) or high (*filled circle*) nutrient conditions. Expression levels were obtained using Western immunoblotting of spheroid homogenates, and the value obtained at the day 2 time point was assigned a value of 1.0. All data points correspond to the mean ± SEM obtained from at least three independent spheroid homogenates

preferentially funnelled into provision of biosynthetic precursors. Expression of pyruvate kinase did not vary significantly during the 20-day period, suggesting that the increased capacity was via altered regulation of the enzyme.

Pyruvate may proceed towards further oxidation via the TCA cycle under conditions of sufficient cellular oxygenation. An alternative route is the reduction to lactate via the enzyme lactate dehydrogenase (LDH). A key feature of this reaction is the liberation of NAD^+, which is used in the early reactions of glycolysis. Under oxygenated conditions, NAD^+ is liberated via reactions in the TCA cycle. In hypoxia, or conditions favouring reduced pyruvate kinase activity (e.g. to generate biosynthetic precursors), pyruvate is "shunted" towards lactate.

Tumour spheroids grown under low nutrient conditions displayed no alteration in either the capacity (Fig. 4b) or the relative expression level (Fig. 4d) of LDH during the 20-day growth period. In contrast, the capacity of LDH under high nutrient conditions displayed a positive linear relationship, and the extent of this change was a twofold increase (Fig. 4b). In line with this increase in capacity, the expression level of LDH was elevated, with peak expression at day 12 of the growth period (Fig. 4d).

Maximal Activity Capacity and Expression of Glucose-6-Phosphate Dehydrogenase and Cytosolic Malate Dehydrogenase During Tumour Spheroid Growth

Glycolytic metabolism is not as efficient as oxidative pathways; however, it does provide a number of biosynthetic precursors that are vital to support tissue growth. For example, during periods of high glycolytic flux, a proportion of glucose-6-phosphate passes through the pentose-phosphate pathway. The PPP provides ribose sugars that are components of cellular nucleotides, whose availability is important to rapidly growing tumours. In addition, the PPP is a source of the reduced cofactor NADPH, which is used predominantly by the cytosolic biosynthetic pathways, and these are also vital for growing tissue.

The entry point for the complete PPP is the oxidation of glucose-6-phosphate to 6-phosphoglucono-δ-lactone, which provides NADPH and is catalysed by glucose-6-phosphate dehydrogenase (G6PDH). The cellular capacity

of G6PDH in spheroids grown under low nutrient conditions did not vary significantly during the 20-day growth period (Fig. 5a). During this period, there was a minor increase in the relative expression level of the enzyme (Fig. 5c). Under high nutrient conditions, the G6PDH capacity rose in a linear fashion during the first 15 days, which corresponded to the period of greatest spheroid growth and glucose consumption. There was an increase in the relative expression level of the enzyme during the first 6 days, and this elevated level remained relatively constant throughout the period of 20 days. However, the G6PDH capacity of the spheroids fell during the last 5 days of the investigative period without a marked alteration in expression. The lack of correlation between enzyme capacity and expression level indicates that post-translational modification of G6PDH is the dominant control mechanism.

Malate dehydrogenase (MDH) occurs within the mitochondrial matrix and the cytosol and serves as a key enzyme in regulating the flux of bioenergetic intermediates. Malate may be reduced to oxaloacetate by MDH in the cytosol, which may subsequently generate aspartate and a number of nitrogen containing metabolites including pyrimidines. The MDH capacity in spheroids grown under low nutrient conditions did not alter significantly from that demonstrated at day 2 (Fig. 5b). The extent of this change presumably reflects the lack of growth, and need for biosynthetic precursors, under the fuel depleted conditions. Under high nutrient conditions, the MDH capacity exhibited a biphasic profile during the growth period (Fig. 5b). The capacity increased during the rapid phase of growth between days 10 and 15, which is a period of high requirement for biosynthetic precursors, particularly nitrogen containing nucleotides. Altered expression of MDH was not responsible for the capacity changes given the lack of any statistically significant alteration during the growth period (Fig. 5d).

Discussion

Growing tumours are characterised by high proliferative capacity and the ability to invade and metastasise [30]. Tumours display a haphazard architecture and exist in a hostile microenvironment. Consequently, cancer cells undergo considerable adaptive changes during growth. A prime example is the alteration of nutrient fuel metabolism to meet cellular need and function [2, 6, 11, 15]. There are a complex set of influences on tumour cells to ensure such

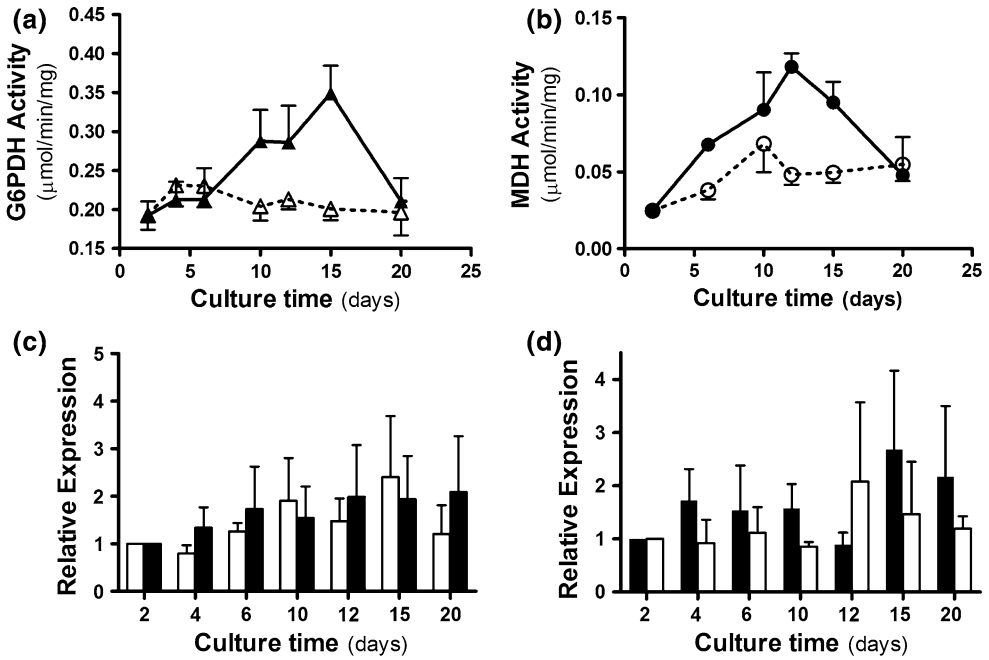

Fig. 5 Activities and expression levels of enzymes involved in cytosolic metabolic links, The activities of **a** glucose-6-phosphate dehydrogenase and **b** malate dehydrogenase were measured at the times indicated in the growth curve of spheroids grown under low (*open circle*) or high (*filled circle*) nutrient conditions. Enzyme activities were determined using coupled assay systems and spectrophotometric determination of NAD(P)H appearance or utilisation. The spectrophotometric data were expressed as μmol/min/mg protein. The relative expression levels of **c** glucose-6-phosphate dehydrogenase and **d** malate dehydrogenase were measured at the times indicated in the growth curve of spheroids grown under low (*open square*) or high (*filled square*) nutrient conditions. Expression levels were obtained using Western immunoblotting of spheroid homogenates, and the value obtained at the day 2 time point was assigned a value of 1.0. All data points correspond to the mean ± SEM obtained from at least three independent spheroid homogenates

adaptive responses. These include transcription factors such as HIF-1 and c-Myc, which alter the protein expression profile [2]. Hormones and signalling networks produce allosteric modulators and activate protein kinases; both of which may alter the activity or stability of metabolic enzymes [2, 6]. Finally, environmental factors such as hypoxia and acidity may alter enzymes directly or by engaging signalling pathways [31–33].

These complex set of factors will dictate the fate of nutrient fuels and the extent of flux through specific pathways; all of which is achieved through modulation of enzyme activity or expression. The present investigation detailed overall glucose consumption and its propensity to divert to lactate production in the tumour spheroid model. Figure 6 shows a summary of the approach and the specific enzyme activities measured to reveal the net flux of glucose during spheroid growth. In addition, properties of key metabolic enzymes were described by measuring expression levels and the maximal activity, hitherto referred to as the capacity. It is important to note that on its own, the capacity parameter does not indicate flux through the specific reaction. It does, however, indicate whether the cell may be capable of responding to increased (or decreased) flux through a particular reaction or pathway. Measuring the enzyme capacity in a tissue homogenate will ascertain whether the enzyme exists in an activated or repressed state. The combination of measuring enzyme capacity and expression may also reveal information regarding the regulation (e.g. posttranslational) of enzyme activity.

The cellular capacity of hexokinase (HK) was increased (under nutrient-rich conditions) during the period between days 6 and 15. However, there was no significant effect on the expression levels of HK. These two observations suggest that post-translational or bioenergetic factors were important factors in the elevation of its capacity in spheroid homogenates. There are four isoforms of HK (I-IV) [34], and the predominant form in cancer cells is HKII [35, 36]. Unlike glucokinase (i.e. HKIII), HKII is associated with the mitochondrial membrane via protein interaction with VDAC [35, 37, 38]. The activity of HKII is sensitive to the association with VDAC at the mitochondrial membrane, and this is further influenced by the phosphorylation status of VDAC [39]. The conformation of HKII and the cholesterol content of the membrane will also influence its insertion into the mitochondrial membrane [40]. The Akt kinase promotes binding of HKII to the mitochondrial membrane by a mechanism thought to involve the increased uptake of glucose. The Akt protein has also been implicated in phosphorylating VDAC, which is known to promote association with HKII [39]. These cellular factors are likely to account for the higher capacity of HKII in our system.

Following a lag period, or minor elevation, the metabolic capacity of PFK-1 activity displayed a considerable rise between days 10 and 15, which corresponded to the mid-log phase of spheroid growth. The expression levels of PFK-1 were not altered to a major extent and demonstrated a progressive reduction during spheroid growth. The

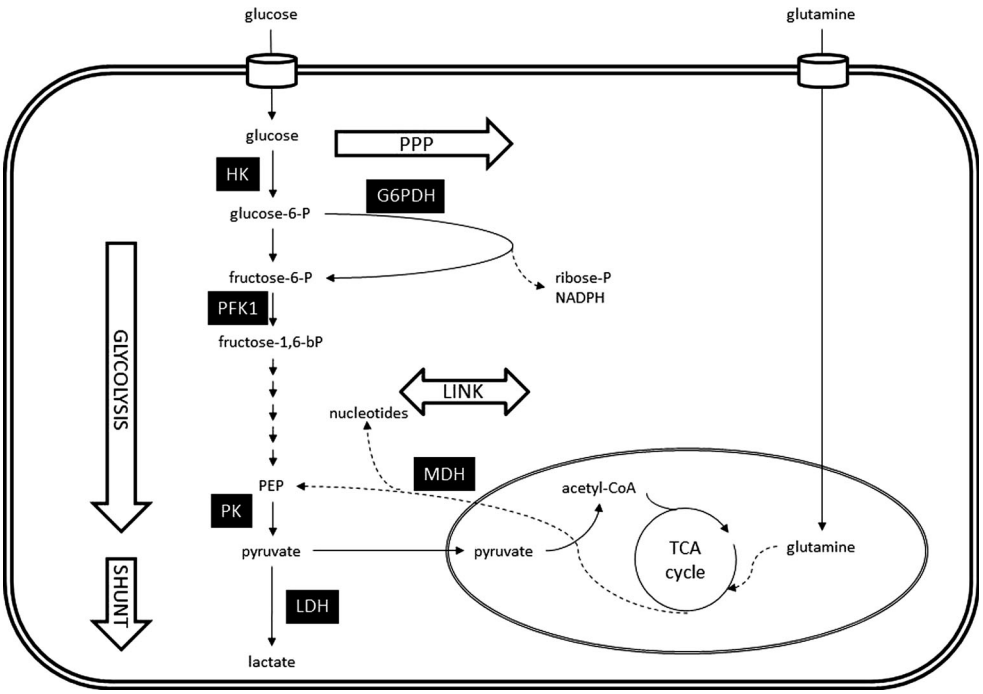

Fig. 6 Summary of the overall strategy used in the present investigation. The diagram demonstrates the flux of glucose in a model cell through glycolysis and the pentose-phosphate pathway. The link to mitochondrial oxidative pathways and the "anaerobic shunt" to lactate production are also shown

expression level of PFK-1 mRNA is elevated in cancer cells [5, 41]; however, there are no alterations specific to stages of tumour development. The lack of correlation between expression level and capacity is explained by the mechanisms of PFK-1 regulation. PFK-1 provides the first committed step in glycolysis and catalyses an irreversible reaction; thereby its activity sets the pace of glycolysis [41, 42]. Predictably, its activity is sensitive to the ratio of [ATP] to [ADP] [43]. However, the dominant regulatory mechanism is through the allosteric activator fructose-2,6-bis-phosphate (F2,6bP) [5, 43]. This potent modulator is formed by the bifunctional enzyme 6-phosphofructo-2-kinase/fructose-2,6-bisphosphatase (PFKFB), which catalyses the formation or degradation of F2,6bP [44, 45]. The precise direction of PFKFB activity is determined by its phosphorylation status. In cancer cells, the highly expressed PFKFB3 isoform is regulated by transcription, post-translational activation and degradation rate [46–48]. HIF-1 has been shown to induce transcription of PFKFB, and its phosphorylation state is sensitive to a number of important signalling kinases in cancer cells (e.g. AKT and AMP-activated kinase) [49–51]. A p53-inducible protein, TIGAR, has also been shown to display F2,6bP activity [52]. Over-expression of TIGAR results in lower activity of PFK-1 and thereby slows down glycolysis in favour of the PPP. The expression of TIGAR is also controlled by factors such as hypoxia in cancer cells [53]. Therefore, the balance between expression of TIGAR and PFKFB3 will dictate the activity of PFK-1 and the direction of glucose flux.

The maximal capacity of pyruvate kinase was gradually increased to a peak at day 12 of the nutrient-rich culture. However, the increased capacity was not associated with an alteration of the expression level. This suggested that a number of post-translational influences were responsible for the increased capacity during spheroid growth. Four isoforms of PYK exist in mammals, and the M2 form is expressed in cancer cells (for review see [54, 55]). PYK-M2 may form a low activity dimeric unit or a high-activity tetrameric form dependent on the tissue type and metabolic requirements [56, 57]. A number of cellular factors have been implicated in shunting PYK-M2 between the two oligomeric forms. For example, tyrosine phosphorylation of PYK-M2 has been demonstrated to disrupt the active tetramer to generate the lower activity dimeric assembly [57]. Fructose-1,6-bisphosphate (F-1,6bP) binds directly to dimeric PYK-M2 and induces formation of the active tetramer [58–60]. F-1,6bP is used in most tissues to allosterically activate PYK in order to elevate the glycolytic rate during periods of high glucose uptake. There are also numerous oncogenic proteins known to interact with PYK-M2 and shift the oligomeric profile between the dimeric and tetrameric forms (see Table 2, [54]). These include tyrosine and serine kinases that alter the phosphorylation status or those that perturb the oligomeric structure via direct interaction with PM-M2 (e.g. T_3). Thus, the oligomeric organisation of PYK-M2 represents a dynamic equilibrium that shifts from high to low activity dependent on whether glucose flux is required for energy production or biosynthetic precursor supply.

During the peak growth phase of spheroids, the metabolic capacity of glucose-6-phosphate dehydrogenase (G6PDH) rose in a linear manner. The doubling of the metabolic capacity was matched by a similar level of increase in enzyme expression under nutrient-replete conditions. G6PDH catalyses the first and irreversible step in the PPP, which is known to be the rate-limiting step [61, 62]. Flux through the PPP is determined by the cellular requirement for NADPH and ribose-5-phosphate [63]. The cellular ratio of $NADPH/NADP^+$ provides short-term allosteric control of G6PDH [64]. It has been widely demonstrated that many cancer types display increased expression of G6PDH and has even been viewed as a hallmark feature [65, 66]. The list of factors, signals and transduction pathways that influence the expression or location of G6PDH is significant (see Table 1, [63]). In addition to the cellular redox status, it is cell-cycle regulators (p53 and ATM) and cell stress response elements (HIF-1 and AMPK) that are likely to mediate altered expression or localisation of G6PDH in solid tumours [67, 68].

Malate dehydrogenase (MDH) is a key “link” enzyme between mitochondrial and cytosolic pools of metabolic intermediates. The MDH capacity in spheroids displayed a biphasic profile with maximal activity during the growth period. Such a profile is in keeping with the cellular role played by this versatile enzyme. For example, the oxidation of glutamine generates several TCA cycle intermediates that may be shuttled from the mitochondrial matrix to the cytoplasm involving conversion to (and from) malate [3, 69]. TCA cycle intermediates may then be utilised as biosynthetic precursors for lipids, purines and pyrimidines, all of whom are important in generating biomass for proliferating tissues [2, 11, 15]. MDH activity may also be employed to generate NADPH, which is a key cofactor in biosynthetic pathways and for free radical scavenging.

Glucose metabolism was also investigated under conditions of nutrient deprivation that were achieved by not replenishing growth medium. Under these conditions, the growth rate of the spheroids was greatly reduced, reflecting the key role of glucose (and glutamine) in sustaining cellular energy and biomass for proliferation. As anticipated, the glucose concentration of the medium was rapidly reduced, thereby leading to a marked diminution of consumption. Lactate accumulation was sustained to day 12 and associated with a commensurate steady acidification of the circulating growth medium. The continued production

of lactate despite the reduction in available glucose is likely to arise through the catabolism of other fuels or the breakdown of cellular macromolecules. The accumulation of lactate was mirrored by a steady accumulation of the growth medium due to cellular expulsion of acidic compounds including lactate. The source of lactate in the culture medium (i.e. peripheral or central cells) remains a difficult issue to resolve. However, the proposal by Feron [69] of a "lactate cycle" between layers of a tumour suggests that lactate observed in culture medium emanates from deeper layers of the tissue.

In contrast to the observations with nutrient-replete medium, there were relatively few alterations to the expression levels of glycolytic enzymes or their cellular capacity. A previous manuscript has indicated that glucose depletion leads to increased mRNA levels for GLUT1 and the PFKB3 isoform [70]. There were no data available on protein expression or the activity of these enzymes. Our approach was to investigate protein levels and overall capacity of specific enzymes. For example, G6PDH plays a key role in the PPP to provide ribose sugars for nucleotide synthesis, and its metabolic capacity was unaltered in spheroid homogenates. This is consistent with the depleted spheroid growth, and its resultant diminished proliferation rate. The capacity of spheroid homogenates for HK and PFK-1 activity did not alter until day 12 when their activities increased significantly. This may reflect the near exhaustion of cellular fuels and the stimulus (e.g. by increasing [ADP] levels) to optimise the potential activities of these pace-setting glycolytic enzymes.

The present investigation focussed on protein expression levels and the overall catalytic capacity in spheroids during the entire growth period. We, and others, have detailed the complex and dynamic alterations in spheroid morphology throughout this growth period [27–29, 71–73]. These include the formation of a quiescent pool of cells and a proportionally decreasing fraction of proliferating cells. As the spheroid growth proceeds, the central region assumes a hypoxic environment that is deficient in nutrients and growth factors. In the final stages of spheroid growth, a central necrotic core develops in response to the lack of oxygen, nutrient deficiency and build-up of toxic metabolites. The alterations in cellular characteristics are produced by environmental factors including low oxygenation and insufficient nutrient availability. In the present manuscript, the changes in microenvironment and cell state are "averaged" and include myriad factors. In a subsequent investigation, we have trapped TS in hypoxic conditions or in a state of quiescence. Hypoxic TS displayed elevated glycolytic flux, whereas quiescence led to a depressed flux (*data not shown*). These observations reveal the complex and often distinct influences found within a solid tumour mass.

The investigations have revealed that the flux of glucose through glycolysis, the PPP and either shunting to lactate or entry to the TCA cycle is governed by a complex set of control processes. These include allosteric modulators, post-translational modifications and transcriptions. The investigations have provided insight into whether enzyme activity or its expression profile is likely to be the primary influence in setting its overall influence. Future investigations will focus on specific individual microenvironmental factors and their effects on enzyme activity and the fluxes of key nutrients.

References

1. Warburg, O. (1956). On the origin of cancer cells. *Science, 123*, 309–314.
2. Ward, P. S., & Thompson, C. B. (2012). Metabolic reprogramming: a cancer hallmark even Warburg did not anticipate. *Cancer Cell, 21*, 297–308.
3. DeBerardinis, R. J., Mancuso, A., Daikhin, E., Nissim, I., Yudkoff, M., Wehrli, S., et al. (2007). Beyond aerobic glycolysis: transformed cells can engage in glutamine metabolism that exceeds the requirement for protein and nucleotide synthesis. *Proceedings of the National Academy of Sciences of the United States of America, 104*, 19345–19350.
4. Fantin, V. R., & Leder, P. (2006). Mitochondriotoxic compounds for cancer therapy. *Oncogene, 25*, 4787–4797.
5. Moreno-Sanchez, R., Rodriguez-Enriquez, S., Marin-Hernandez, A., & Saavedra, E. (2007). Energy metabolism in tumor cells. *FEBS Journal, 274*, 1393–1418.
6. Vander Heiden, M. G., Cantley, L. C., & Thompson, C. B. (2009). Understanding the Warburg effect: the metabolic requirements of cell proliferation. *Science, 324*, 1029–1033.
7. Weinhouse, S. (1976). The Warburg hypothesis fifty years later. *Journal of Cancer Research and Clinical Oncology. Cancer Research and Clinical Oncology, 87*, 115–126.
8. Gottschalk, S., Anderson, N., Hainz, C., Eckhardt, S. G., & Serkova, N. J. (2004). Imatinib (STI571)-mediated changes in glucose metabolism in human leukemia BCR-ABL-positive cells. *Clinical Cancer Research, 10*, 6661–6668.
9. Nolop, K. B., Rhodes, C. G., Brudin, L. H., Beaney, R. P., Krausz, T., Jones, T., et al. (1987). Glucose utilization in vivo by human pulmonary neoplasms. *Cancer, 60*, 2682–2689.
10. Chen, J. Q., & Russo, J. (2012). Dysregulation of glucose transport, glycolysis, TCA cycle and glutaminolysis by oncogenes and tumor suppressors in cancer cells. *Biochimica et Biophysica Acta, 1826*, 370–384.
11. Israel, M., & Schwartz, L. (2011). The metabolic advantage of tumor cells. *Molecular Cancer, 10*, 70.
12. Dang, C. V., Le, A., & Gao, P. (2009). MYC-induced cancer cell energy metabolism and therapeutic opportunities. *Clinical Cancer Research, 15*, 6479–6483.
13. Li, F., Wang, Y., Zeller, K. I., Potter, J. J., Wonsey, D. R., O'Donnell, K. A., et al. (2005). Myc stimulates nuclearly encoded mitochondrial genes and mitochondrial biogenesis. *Molecular and Cellular Biology, 25*, 6225–6234.
14. Talks, K. L., Turley, H., Gatter, K. C., Maxwell, P. H., Pugh, C. W., Ratcliffe, P. J., et al. (2000). The expression and distribution of the hypoxia-inducible factors HIF-1alpha and HIF-2alpha in normal human tissues, cancers, and tumor-associated macrophages. *American Journal of Pathology, 157*, 411–421.
15. Dang, C. V. (2010). Glutaminolysis: supplying carbon or nitrogen or both for cancer cells? *Cell Cycle, 9*, 3884–3886.

16. Semenza, G. L. (2009). Regulation of cancer cell metabolism by hypoxia-inducible factor 1. *Seminars in Cancer Biology, 19*, 12–16.
17. Semenza, G. L., Roth, P. H., Fang, H. M., & Wang, G. L. (1994). Transcriptional regulation of genes encoding glycolytic enzymes by hypoxia-inducible factor 1. *Journal of Biological Chemistry, 269*, 23757–23763.
18. Bensaad, K., Tsuruta, A., Selak, M. A., Vidal, M. N., Nakano, K., Bartrons, R., et al. (2006). TIGAR, a p53-inducible regulator of glycolysis and apoptosis. *Cell, 126*, 107–120.
19. Contractor, T., & Harris, C. R. (2012). p53 negatively regulates transcription of the pyruvate dehydrogenase kinase Pdk2. *Cancer Research, 72*, 560–567.
20. Hu, W., Zhang, C., Wu, R., Sun, Y., Levine, A., & Feng, Z. (2010). Glutaminase 2, a novel p53 target gene regulating energy metabolism and antioxidant function. *Proceedings of the National Academy of Sciences of the United States of America, 107*, 7455–7460.
21. Primeau, A. J., Rendon, A., Hedley, D., Lilge, L., & Tannock, I. F. (2005). The distribution of the anticancer drug Doxorubicin in relation to blood vessels in solid tumors. *Clinical Cancer Research, 11*, 8782–8788.
22. Swietach, P., Patiar, S., Supuran, C. T., Harris, A. L., & Vaughan-Jones, R. D. (2009). The role of carbonic anhydrase 9 in regulating extracellular and intracellular ph in three-dimensional tumor cell growths. *Journal of Biological Chemistry, 284*, 20299–20310.
23. Wykoff, C. C., Beasley, N. J., Watson, P. H., Turner, K. J., Pastorek, J., Sibtain, A., et al. (2000). Hypoxia-inducible expression of tumor-associated carbonic anhydrases. *Cancer Research, 60*, 7075–7083.
24. Modok, S., Hyde, P., Mellor, H. R., Roose, T., & Callaghan, R. (2006). Diffusivity and distribution of vinblastine in three-dimensional tumour tissue: Experimental and mathematical modelling. *European Journal of Cancer, 42*, 2404–2413.
25. Tong, R. T., Boucher, Y., Kozin, S. V., Winkler, F., Hicklin, D. J., & Jain, R. K. (2004). Vascular normalization by vascular endothelial growth factor receptor 2 blockade induces a pressure gradient across the vasculature and improves drug penetration in tumors. *Cancer Research, 64*, 3731–3736.
26. Hall, M. D., Martin, C., Ferguson, D. J. P., Phillips, R. M., Hambley, T. W., & Callaghan, R. (2004). Comparative efficacy of novel platinum(IV) compounds with established chemotherapeutic drugs in solid tumour models. *Biochemical Pharmacology, 67*, 17–30.
27. Mellor, H. R., Ferguson, D. J., & Callaghan, R. (2005). A model of quiescent tumour microregions for evaluating multicellular resistance to chemotherapeutic drugs. *British Journal of Cancer, 93*, 302–309.
28. Mellor, H. R., Snelling, S., Hall, M. D., Modok, S., Jaffar, M., Hambley, T. W., et al. (2005). The influence of tumour microenvironmental factors on the efficacy of cisplatin and novel platinum(IV) complexes. *Biochemical Pharmacology, 70*, 1137–1146.
29. Hirschhaeuser, F., Menne, H., Dittfeld, C., West, J., Mueller-Klieser, W., & Kunz-Schughart, L. A. (2010). Multicellular tumor spheroids: an underestimated tool is catching up again. *Journal of Biotechnology, 148*, 3–15.
30. Hanahan, D., & Weinberg, R. A. (2000). The hallmarks of cancer. *Cell, 100*, 57–70.
31. Casciari, J. J., Sotirchos, S. V., & Sutherland, R. M. (1992). Variations in tumor cell growth rates and metabolism with oxygen concentration, glucose concentration, and extracellular pH. *Journal of Cellular Physiology, 151*, 386–394.
32. Vaupel, P., Fortmeyer, H. P., Runkel, S., & Kallinowski, F. (1987). Blood flow, oxygen consumption, and tissue oxygenation of human breast cancer xenografts in nude rats. *Cancer Research, 47*, 3496–3503.
33. Vaupel, P. W., Frinak, S., & Bicher, H. I. (1981). Heterogeneous oxygen partial pressure and pH distribution in C3H mouse mammary adenocarcinoma. *Cancer Research, 41*, 2008–2013.
34. Wilson, J. E. (2003). Isozymes of mammalian hexokinase: structure, subcellular localization and metabolic function. *Journal of Experimental Biology, 206*, 2049–2057.
35. Pastorino, J. G., & Hoek, J. B. (2008). Regulation of hexokinase binding to VDAC. *Journal of Bioenergetics and Biomembranes, 40*, 171–182.
36. Pedersen, P. L., Mathupala, S., Rempel, A., Geschwind, J. F., & Ko, Y. H. (2002). Mitochondrial bound type II hexokinase: a key player in the growth and survival of many cancers and an ideal prospect for therapeutic intervention. *Biochimica et Biophysica Acta, 1555*, 14–20.
37. Bustamante, E., Morris, H. P., & Pedersen, P. L. (1981). Energy metabolism of tumor cells. Requirement for a form of hexokinase with a propensity for mitochondrial binding. *Journal of Biological Chemistry, 256*, 8699–8704.
38. Linden, M., Gellerfors, P., & Nelson, B. D. (1982). Pore protein and the hexokinase-binding protein from the outer membrane of rat liver mitochondria are identical. *FEBS Letters, 141*, 189–192.
39. Pastorino, J. G., Hoek, J. B., & Shulga, N. (2005). Activation of glycogen synthase kinase 3beta disrupts the binding of hexokinase II to mitochondria by phosphorylating voltage-dependent anion channel and potentiates chemotherapy-induced cytotoxicity. *Cancer Research, 65*, 10545–10554.
40. Baggetto, L. G., Clottes, E., & Vial, C. (1992). Low mitochondrial proton leak due to high membrane cholesterol content and cytosolic creatine kinase as two features of the deviant bioenergetics of Ehrlich and AS30-D tumor cells. *Cancer Research, 52*, 4935–4941.
41. Yalcin, A., Telang, S., Clem, B., & Chesney, J. (2009). Regulation of glucose metabolism by 6-phosphofructo-2-kinase/fructose-2,6-bisphosphatases in cancer. *Experimental and Molecular Pathology, 86*, 174–179.
42. Jenkins, C. M., Yang, J., Sims, H. F., & Gross, R. W. (2011). Reversible high affinity inhibition of phosphofructokinase-1 by acyl-CoA: a mechanism integrating glycolytic flux with lipid metabolism. *Journal of Biological Chemistry, 286*, 11937–11950.
43. Hers, H. G., & Van Schaftingen, E. (1982). Fructose 2,6-bisphosphate 2 years after its discovery. *Biochemistry Journal, 206*, 1–12.
44. Okar, D. A., Manzano, A., Navarro-Sabate, A., Riera, L., Bartrons, R., & Lange, A. J. (2001). PFK-2/FBPase-2: maker and breaker of the essential biofactor fructose-2,6-bisphosphate. *Trends in Biochemical Sciences, 26*, 30–35.
45. Rider, M. H., Bertrand, L., Vertommen, D., Michels, P. A., Rousseau, G. G., & Hue, L. (2004). 6-phosphofructo-2-kinase/fructose-2,6-bisphosphatase: head-to-head with a bifunctional enzyme that controls glycolysis. *Biochemistry Journal, 381*, 561–579.
46. Chesney, J., Mitchell, R., Benigni, F., Bacher, M., Spiegel, L., Al-Abed, Y., et al. (1999). An inducible gene product for 6-phosphofructo-2-kinase with an AU-rich instability element: role in tumor cell glycolysis and the Warburg effect. *Proceedings of the National Academy of Sciences of the United States of America, 96*, 3047–3052.
47. Mor, I., Cheung, E. C., & Vousden, K. H. (2011). Control of glycolysis through regulation of PFK1: old friends and recent additions. *Cold Spring Harbor Symposia on Quantitative Biology, 76*, 211–216.
48. Tudzarova, S., Colombo, S. L., Stoeber, K., Carcamo, S., Williams, G. H., & Moncada, S. (2011). Two ubiquitin ligases, APC/C-Cdh1 and SKP1-CUL1-F (SCF)-beta-TrCP, sequentially

regulate glycolysis during the cell cycle. *Proceedings of the National Academy of Sciences of the United States of America, 108*, 5278–5283.
49. Marsin, A. S., Bouzin, C., Bertrand, L., & Hue, L. (2002). The stimulation of glycolysis by hypoxia in activated monocytes is mediated by AMP-activated protein kinase and inducible 6-phosphofructo-2-kinase. *Journal of Biological Chemistry, 277*, 30778–30783.
50. Minchenko, O., Opentanova, I., & Caro, J. (2003). Hypoxic regulation of the 6-phosphofructo-2-kinase/fructose-2,6-bisphosphatase gene family (PFKFB-1-4) expression in vivo. *FEBS Letters, 554*, 264–270.
51. Moon, J. S., Jin, W. J., Kwak, J. H., Kim, H. J., Yun, M. J., Kim, J. W., et al. (2011). Androgen stimulates glycolysis for de novo lipid synthesis by increasing the activities of hexokinase 2 and 6-phosphofructo-2-kinase/fructose-2,6-bisphosphatase 2 in prostate cancer cells. *Biochemistry Journal, 433*, 225–233.
52. Li, H., & Jogl, G. (2009). Structural and biochemical studies of TIGAR (TP53-induced glycolysis and apoptosis regulator). *Journal of Biological Chemistry, 284*, 1748–1754.
53. Kimata, M., Matoba, S., Iwai-Kanai, E., Nakamura, H., Hoshino, A., Nakaoka, M., et al. (2010). p53 and TIGAR regulate cardiac myocyte energy homeostasis under hypoxic stress. *American Journal of Physiology. Heart and Circulatory Physiology, 299*, H1908–H1916.
54. Mazurek, S. (2011). Pyruvate kinase type M2: a key regulator of the metabolic budget system in tumor cells. *International Journal of Biochemistry & Cell Biology, 43*, 969–980.
55. Tamada, M., Suematsu, M., & Saya, H. (2012). Pyruvate kinase m2: multiple faces for conferring benefits on cancer cells. *Clinical Cancer Research, 18*, 5554–5561.
56. Christofk, H. R., Vander Heiden, M. G., Harris, M. H., Ramanathan, A., Gerszten, R. E., Wei, R., et al. (2008). The M2 splice isoform of pyruvate kinase is important for cancer metabolism and tumour growth. *Nature, 452*, 230–233.
57. Hitosugi, T., Kang, S., Vander Heiden, M. G., Chung, T. W., Elf, S., Lythgoe, K., et al. (2009). Tyrosine phosphorylation inhibits PKM2 to promote the Warburg effect and tumor growth. *Science Signal, 2*, ra73.
58. Ashizawa, K., Willingham, M. C., Liang, C. M., & Cheng, S. Y. (1991). In vivo regulation of monomer-tetramer conversion of pyruvate kinase subtype M2 by glucose is mediated via fructose 1,6-bisphosphate. *Journal of Biological Chemistry, 266*, 16842–16846.
59. Christofk, H. R., Vander Heiden, M. G., Wu, N., Asara, J. M., & Cantley, L. C. (2008). Pyruvate kinase M2 is a phosphotyrosine-binding protein. *Nature, 452*, 181–186.
60. Dombrauckas, J. D., Santarsiero, B. D., & Mesecar, A. D. (2005). Structural basis for tumor pyruvate kinase M2 allosteric regulation and catalysis. *Biochemistry, 44*, 9417–9429.
61. Kletzien, R. F., Harris, P. K., & Foellmi, L. A. (1994). Glucose-6-phosphate dehydrogenase: a "housekeeping" enzyme subject to tissue-specific regulation by hormones, nutrients, and oxidant stress. *FASEB Journal, 8*, 174–181.
62. Wood, T. (1986). Physiological functions of the pentose phosphate pathway. *Cell Biochemistry and Function, 4*, 241–247.
63. Stanton, R. C. (2012). Glucose-6-phosphate dehydrogenase, NADPH, and cell survival. *IUBMB Life, 64*, 362–369.
64. Holten, D., Procsal, D., & Chang, H. L. (1976). Regulation of pentose phosphate pathway dehydrogenases by NADP +/ NADPH ratios. *Biochemical and Biophysical Research Communications, 68*, 436–441.
65. Boros, L. G., Brandes, J. L., Yusuf, F. I., Cascante, M., Williams, R. D., & Schirmer, W. J. (1998). Inhibition of the oxidative and nonoxidative pentose phosphate pathways by somatostatin: a possible mechanism of antitumor action. *Medical Hypotheses, 50*, 501–506.
66. Frederiks, W. M., Bosch, K. S., Hoeben, K. A., van Marle, J., & Langbein, S. (2010). Renal cell carcinoma and oxidative stress: The lack of peroxisomes. *Acta Histochemica, 112*, 364–371.
67. Cosentino, C., Grieco, D., & Costanzo, V. (2011). ATM activates the pentose phosphate pathway promoting anti-oxidant defence and DNA repair. *EMBO Journal, 30*, 546–555.
68. Jiang, P., Du, W., Wang, X., Mancuso, A., Gao, X., Wu, M., et al. (2011). p53 regulates biosynthesis through direct inactivation of glucose-6-phosphate dehydrogenase. *Nature Cell Biology, 13*, 310–316.
69. Feron, O. (2009). Pyruvate into lactate and back: from the Warburg effect to symbiotic energy fuel exchange in cancer cells. *Radiotherapy and Oncology, 92*, 329–333.
70. Yun, H., Lee, M., Kim, S. S., & Ha, J. (2005). Glucose deprivation increases mRNA stability of vascular endothelial growth factor through activation of AMP-activated protein kinase in DU145 prostate carcinoma. *Journal of Biological Chemistry, 280*, 9963–9972.
71. Friedrich, J., Ebner, R., & Kunz-Schughart, L. A. (2007). Experimental anti-tumor therapy in 3-D: spheroids-old hat or new challenge? *International Journal of Radiation Biology, 83*, 849–871.
72. Kunz-Schughart, L. A., Groebe, K., & Mueller-Klieser, W. (1996). Three-dimensional cell culture induces novel proliferative and metabolic alterations associated with oncogenic transformation. *International Journal of Cancer, 66*, 578–586.
73. Rodriguez-Enriquez, S., Gallardo-Perez, J. C., Aviles-Salas, A., Marin-Hernandez, A., Carreno-Fuentes, L., Maldonado-Lagunas, V., et al. (2008). Energy metabolism transition in multi-cellular human tumor spheroids. *Journal of Cellular Physiology, 216*, 189–197.